Journal of Integrative Neuroscience

*J. Integr. Neurosci.* **2026**; 25(6): 49659
https://doi.org/10.31083/JIN49659

*Original Research*

# Small Extracellular Vesicles Derived From Mesenchymal Stem Cells Exert Neuroprotective Effect Against a Model of Dopamine Dysfunction by Inhibiting Caspase-8/Caspase-3-Mediated Apoptosis

Songzhe He[1,2,3,4], Qi Qu[5], Ling Hu[6], Yufang Yan[6], Qiongqiong Wang[1,2,3], Yi Ouyang[6], Xiaofang Wang[7,8], Shaogang Qu[6,*]

[1]Department of Neurology, Nanfang Hospital, Southern Medical University, 510515 Guangzhou, Guangdong, China
[2]Key Laboratory of Mental Health of the Ministry of Education, Southern Medical University, 510515 Guangzhou, Guangdong, China
[3]Guangdong-Hong Kong-Macao Greater Bay Area Center for Brain Science and Brain-Inspired Intelligence, 510515 Guangzhou, Guangdong, China
[4]Department of Clinic Laboratory, The First Affiliated Hospital of Guilin Medical University, 541001 Guilin, Guangxi, China
[5]Department of Neurobiology, School of Basic Medical Sciences, Southern Medical University, 510515 Guangzhou, Guangdong, China
[6]Department of Neurology, Ganzhou Hospital-Nanfang Hospital, Southern Medical University, 341000 Ganzhou, Jiangxi, China
[7]ImStem Biotechnology, Inc., Farmington, CT 06030, USA
[8]ZhuHai Hengqin ImStem Biotechnology Co., Ltd., 519000 Zhuhai, Guangdong, China
*Correspondence: sgq9528@smu.edu.cn (Shaogang Qu)
Academic Editor: François Ichas
Submitted: 2 January 2026 Revised: 23 March 2026 Accepted: 31 March 2026 Published: 22 June 2026

**Abstract**

**Background**: The precise pathological mechanisms driving Parkinson's disease (PD) progression remain incompletely understood, and there are currently no therapies that can modify the course of the disease. While mesenchymal stem cells (MSCs) hold therapeutic potential for various conditions, their clinical utility is constrained by challenges in sourcing and limited availability. **Methods**: This study investigated a novel therapeutic approach using trophoblast-derived mesenchymal-like stem cells (T-MSCs), which can be stably generated from commercially available embryonic stem cells, and the small extracellular vesicles (T-MSCs-sEVs) that they secrete. We explored the therapeutic effects against PD by inhibiting Caspase-8/Caspase-3-mediated apoptosis both *in vitro* and *in vivo* using experimental assays (e.g., flow cytometry (FCM) analysis, western blotting, and immunofluorescence staining). **Results**: The selected cytokine Clusterin was validated via G-Series Mouse Cytokine Antibody Array 4000 (GSM-CAA-4000) using ELISA kits, which revealed its involvement in apoptosis during the PD process. Moreover, T-MSCs and T-MSCs-sEVs could alleviate dopaminergic (DA) neuron damage *in vitro* and *in vivo* by inhibiting the Caspase-8/Caspase-3-mediated apoptotic pathway. **Conclusions**: The results suggest that T-MSCs-sEVs represent a promising biological candidate for future therapeutic strategies aimed at treating PD.

**Keywords:** Parkinson's disease; dopaminergic neuron; mesenchymal stem cells; extracellular vesicles; apoptosis

## 1. Introduction

Parkinson's disease (PD) is a progressive neurodegenerative disorder that is characterized by motor impairments such as bradykinesia, resting tremors, and postural instability; this disease predominantly affects the elderly population [1,2,3]. The International Parkinson and Movement Disorder Society describes PD as "a core clinical motor syndrome (Parkinsonism) accompanied by progressing loss of dopaminergic (DA) neurons in the substantia nigra pars compacta (SNpc) and α-synuclein (α-syn) protein accumulation (known as Lewy bodies)" [4,5]. As the population ages, the number of people with PD is increasing, with a particularly steep increase in incidence after the age of 60 [6]. Moreover, the incidence, prevalence, and risk of death are greater in men than in women, resulting in a direct and indirect economic burden on society [7].

Apoptosis, a type of programmed cell death, is primarily characterized by cell shrinkage, chromatin condensation, and DNA fragmentation [8]. In general, apoptosis can be divided into intrinsic (mitochondrial) and extrinsic (death receptor) pathways [9,10]. The intrinsic apoptosis pathway in mitochondria is regulated by pro- and antiapoptotic proteins of the B-cell lymphoma-2 (BCL-2) family [11,12]. In contrast, the extrinsic pathway is initiated by ligands binding to death receptors belonging to the tumor necrosis factor (TNF) receptor superfamily, leading to the activation of Caspase-8 and subsequent execution of apoptosis [13,14]. Furthermore, excessive apoptosis can accelerate the progression of neurodegenerative diseases, including PD. Current evidence identifies DA neuronal apoptosis as a pivotal event in PD pathology, with contributing mechanisms involving α-syn aggregation and related processes [15,16,17]. As highlighted by Pan et al. [18], excessive nuclear translocation of α-syn within hippocampal neurons has been demonstrated to induce DNA damage, which subsequently triggers aberrant cell cycle activation and arrest, which further induces hippocampal neuron apoptosis and an inflammatory response, ultimately leading to cog-

nitive decline in mice. Additionally, research indicates that α-syn aggregation exacerbates neuroinflammation and neuronal apoptosis via the IL6ST-AS/STAT3/HIF-1α axis [19]. Subsequently, it was found that α-syn could promote abnormal cell cycle initiation and induce DA neuron apoptosis by regulating Cyclin D1 [20]. To elucidate the mechanisms underlying the effects on neuronal apoptosis, He S et al. [21] utilized chlorogenic acid (CGA) to alleviate oxidative stress by modulating the Akt/Erk1/2 signaling pathway, thus inhibiting neuronal apoptosis in PD. It has also been shown that telmisartan could control mitochondrial function, gait, and neuronal apoptosis in a 1-Methyl-4-phenyl-1,2,3,6-tetrahydropyridine hydrochloride (MPTP)-induced PD model through activation of the Akt/GSK3β/PGC1α pathway [22]. Meanwhile, rubusoside, which is the primary component of Chinese sweet leaf, was confirmed to mitigate neuroinflammation and cellular apoptosis by inhibiting the JNK/p38 MAPK/NF-κB signaling pathway in PD [23]. Hence, to elucidate the mechanisms underlying DA neuron loss in PD, it is essential to understand the various programmed cell death pathways, including apoptosis and autophagic cell death.

Clusterin is a secreted chaperone protein expressed in various tissues, including the heart, brain, and kidneys, and participates in processes such as lipid transport, apoptosis, oxidative stress, and the inflammatory response [24,25,26]. Its expression and function differ across different disease states, including cancer, neurodegenerative diseases, cardiovascular diseases and kidney diseases, exhibiting distinct patterns of alteration [27]. A study has demonstrated elevated clusterin levels in the cerebrospinal fluid of PD patients, suggesting CSF clusterin levels might serve as a potential marker for PD [28]. However, further exploration is required to elucidate how Clusterin regulates apoptosis in PD pathogenesis.

Mesenchymal stem cells (MSCs) are non-hematopoietic, pluripotent cells obtained from several tissues. They have the potential for self-renewal, regulation of immune function, and anti-inflammatory abilities [29,30,31]. MSCs are well known to mediate antiapoptotic effects across various organs through two principal pathways. First, the secretion of multiple growth factors facilitates cell regeneration and tissue repair. Second, by inducing transcription or transferring mRNA or miRNA associated with cell proliferation to damaged cells, the expression of regenerative/antiapoptotic genes can be promoted. It has been reported that exosomes derived from human umbilical cord mesenchymal stem cells (hucMSCs-Exos) could be used to suppress the initiation of apoptosis in 6-OHDA-stimulated SH-SY5Y cells [32]. Similarly, exosomes isolated from GA pretreated Wharton's Jelly-derived mesenchymal stem cells (WJMSCs) could reduce the expression of apoptosis-related proteins induced by 6-OHDA, further improving mitochondrial dysfunction and resulting in neuroprotective effects [33]. In addition, hucMSCs-Exos loaded with brain-derived neurotrophic factor (BDNF-EXO) have been found to effectively suppress 6-OHDA-induced apoptosis and ferroptosis in SH-SY5Y cells [34]. Despite their extensive use in preclinical research for various human diseases, the clinical application of MSCs has been limited by their scarce availability and insufficient quantities. Our previous report confirmed that special mesenchymal-like stem cells (T-MSCs) obtained from the trophoblast stage of commercially available embryonic stem cells can display the characteristics of multipotent MSCs [35]. Furthermore, after purification and identification, the small extracellular vesicles secreted by T-MSCs (T-MSCs-sEVs) can cross the blood–brain barrier (BBB) and be taken up by DA neurons in an endocytic manner, demonstrating the antioxidant effect on PD through the Keap1-Nrf2-SOD pathway. Thus, we investigated whether T-MSCs contributed to antiapoptotic molecular mechanisms involving small extracellular vesicles in PD.

Currently, no Food and Drug Administration (FDA)-approved disease-modifying therapies are available for PD. This study evaluated the recovery of DA neuron damage and apoptosis in the PD model following treatment with T-MSCs or T-MSCs-sEVs. The data showed that T-MSCs or T-MSCs-sEVs had therapeutic effects on PD by inhibiting Caspase-8/Caspase-3 signaling-mediated apoptosis both *in vitro* and *in vivo*. The findings indicate that T-MSCs-sEVs play a crucial role in protecting DA neurons, highlighting their potential as a future biological agent for PD treatment.

## 2. Materials and Methods

### *2.1 Antibodies and Reagents*

The following antibodies and reagents were utilized in this study: mouse Clusterin ELISA kit (Boster, EK0923, Wuhan, Hubei, China), anti-Caspase-8 (1:1000, ab25901, Abcam, Boston, MA, USA), anti-Cleaved caspase-3 (1:1000, ab214430, Abcam), anti-Bax (1:1000, ab32503, Abcam), anti-Bcl-2 (1:1000, ab182858, Abcam), anti-Caspase-3 (1:500, sc-7272, Santa Cruz, Dallas, TX, USA), anti-actin (1:1000, AA128, Beyotime, Shanghai, China), HRP-conjugated goat anti-mouse secondary antibody (1:1000, A0216, Beyotime), HRP-conjugated goat anti-rabbit secondary antibody (1:1000, A0208, Beyotime), anti-Alexa Fluor 488-conjugated goat anti-mouse (1:200, BA1126, Boster), DAPI (ab104139, Abcam), MPTP (orb363933-1g, hydrochloride, Biorbyt, Cambridge, UK), $MPP^+$ (D048-1G, Sigma-Aldrich, St. Louis, MO, USA), and an annexin V-FITC apoptosis detection kit (C1062M, Beyotime).

### *2.2 T-MSCs Identification and Analysis of T-MSCs-sEVs Extraction*

T-MSCs were obtained from ImStem Biotechnology, Inc. (Farmington, CT, USA), with all procedures adhering to the National Institutes of Health Guidelines for Human

Stem Cell Research, and tested negative for mycoplasma. In our study, T-MSCs were derived from commercially available ESI−053 embryonic stem cells. As previously described [35], MSCs were cultured, phenotypically identified, and differentiated into three lineages. Similarly, the specific extraction and identification processes of exosomes follow those of our previous report [35].

### *2.3 MN9D Cell Culture*

The cell line (MN9D) used in this study was obtained from the American Type Culture Collection (ATCC, Manassas, VA, USA), with Short Tandem Repeat (STR) identification supplied by Shanghai Biowing Applied Biotechnology Co., Ltd. (Shanghai, China), tested negative for mycoplasma, and cultured in DMEM medium (C11995500BT, Gibco, CA, USA) supplemented with 10% fetal bovine serum (A5669701, Gibco) and 1% penicillin/streptomycin/amphotericin B (P7630, solarbio, Beijing, China) in an incubator at 37 °C and 5% $CO_2$. Standard cell culture techniques were applied once the cells reached 80% confluence. Following stimulation with $MPP^+$, the cells were collected for subsequent experiments.

### *2.4 Cell Viability Assay*

MN9D cells (approx. $1.5 \times 10^3$ cells/mL) were plated in 96-well flat-bottom plates (TCP010096, JET, Shanghai, China). After allowing the cells to adhere, various concentrations of $MPP^+$ were introduced and co-incubated with the cells at 37 °C with 5% $CO_2$ for 24 h. On the second day, 10 µL of CCK-8 solution (K1146, Bimake, Shanghai, China) was added to each well and incubated for an additional 2 h, following the manufacturer's guidelines. Absorbance at 450 nm was subsequently measured using a microplate reader (Infinite 200 Pro, Tecan, Männedorf, Switzerland). All experiments were independently replicated at least three times.

### *2.5 In Vivo Experimental Design and Drug Administration*

This study obtained 6–8-week-old C57BL/6 male mice (weighing 22–25 g) from Zhejiang Vital River Laboratory Animal Technology Co., Ltd. (Jiaxing, Zhejiang, China). Mice were housed in conditions that supported their natural circadian rhythms, with unrestricted access to food and water.

Following a one-week acclimation period, the mice were randomly allocated to different treatment groups. All specific manipulations were carried out as outlined in previous studies [35]. In brief, for T-MSCs treatment, the mice were randomly assigned to four groups: a control group, a T-MSCs group, an MPTP group, and an MPTP + T-MSCs group (n = 10 per group). The MPTP and MPTP + T-MSCs groups received intraperitoneal injections of MPTP (25 mg/kg; Biorbyt) twice weekly over a 5-week period, while the other groups received intraperitoneal injection of an isovolumetric 1× PBS. Subsequently, the T-MSCs and MPTP + T-MSCs groups were intravenously infused with T-MSCs ($5 \times 10^5$ cells/100 µL of PBS) on days 3, 17, and 31 post-modeling, while the remaining groups were injected with 1× PBS. The treated tissues and blood samples were obtained for subsequent analysis. In addition, for T-MSCs-sEVs treatment, the mice were randomly divided into four groups: a control group, a T-MSCs-sEVs group, an MPTP group, and an MPTP + T-MSCs-sEVs group (n = 10 per group). MPTP (25 mg/kg; Biorbyt) was injected intraperitoneally (twice a week for 5 weeks) in the MPTP and MPTP + T-MSCs-sEVs groups, while the other groups received an equal volume of 1× PBS. Following this, the T-MSCs-sEVs and MPTP + T-MSCs-sEVs groups were administered T-MSCs-sEVs ($7.32 \times 10^{10}$ particles/mL) (100 µL per mouse) on days 3, 17, and 31 after modeling, with the remaining groups receiving 1× PBS. Upon completion of the treatment regimen, mice were euthanized with 1% pentobarbital sodium (Cat. No: P3761, Sigma-Aldrich, St. Louis, MO, USA) (40 mg/kg), and tissues and blood were promptly harvested for subsequent analysis of relevant parameters. We randomly selected 3 animals from each experimental group for Western blotting assay. The other animals in the groups were used to provide sufficient biological material for all planned analyses and to confirm the consistency of the observed effects across individuals.

### *2.6 Serum Cytokine Antibody Array*

After the collection of serum samples from the chronic PD mouse model, G-Series Mouse Cytokine Antibody Array 4000 (GSM-CAA-4000, Raybiotech, Guangzhou, Guangdong, China) was used to evaluate the relative levels of 200 cytokines (**Supplementary Table 1**) according to the manufacturer's protocols. Briefly, the glass slide was removed from its box and allowed to air dry completely for 1–2 h. Next, 100 µL of Sample Diluent was added to each well and incubated at 25 °C for 30 min to block slides. The liquid in each well was then discarded, and 60 µL of each sample was added to each well and incubated overnight at 4 °C on a shaker. After washing with 1× wash buffer, each well was incubated with 80 µL of biotinylated antibody at 25 °C on a shaker for 2 h. Next, 80 µL of Cy3-equivalent (QA-CY3E, Raybiotech, Guangzhou, Guangdong, China) dye-conjugated streptavidin was applied and incubated at 25 °C for 1 h after washing. Finally, the signals were visualized using an InnoScan 300 Microarray Scanner (INNOPSYS, Parc dActivité Activestre, Carbonne, France) with the Cy3 wavelength (green channel). Cytokine levels were quantified and analyzed post-normalization using fluorescence signals detected by the Axon GenePix system. Furthermore, Gene Ontology (GO) and Kyoto Encyclopedia of Genes and Genomes (KEGG) analysis were performed to determine the pathways and biological functions of cytokines. Data were enriched using the R package "GO.db" and "ClusterProfiler". The Fisher's exact test was used for enrichment analysis; only pathways with a false discovery rate (FDR) corrected $p < 0.05$ were represented [36].

*2.7 Enzyme-Linked Immunosorbent Assay (ELISA)*

The concentration of the cytokine Clusterin in mouse serum was measured using an ELISA kit according to the manufacturer's instructions. Briefly, 100 µL of either serially diluted standard proteins or mouse serum samples were added to each well and incubated at 37 °C for 1.5 h. Then, 100 µL of biotinylated antibody working solution was added and incubated at 37 °C for 1 h. After washing the wells three times with 1× wash buffer, 100 µL of avidin-biotin-peroxidase complex (ABC) was added. Following a 30 min incubation and five additional washes with 1× wash buffer, 90 µL of Tetramethylbenzidine (TMB) substrate was applied and incubated for 15–20 min at 37 °C in the dark. Finally, 100 µL of stopping solution was added, and absorbance was measured at 450 nm. The absolute levels of clusterin in serum samples were determined by calculation based on a standard curve. The replicates represent biological replicates (n = 3 per group).

*2.8 Apoptosis Analysis*

Apoptosis was assessed using Annexin V staining and flow cytometry (FCM) analysis. The experiments were performed according to our previous publications [37]. Briefly, the cells were cultured in 6-well plates at a density of $5 \times 10^5$ cells/well for 24 h based on the manufacturer's instructions. The cells were washed with 1× PBS, collected using trypsin without EDTA (15050-065, Gibco, CA, USA), and centrifuged at 800 rpm for 5 min. After centrifugation, 195 µL of annexin V-FITC binding solution was added to the cell resuspension. Next, 5 µL of annexin V-FITC was added to the cells and gently mixed evenly. Upon incubation in the dark for 15 min at 25 ℃, the cells were gently mixed with 10 µL of propidium iodide (PI) and incubated for an additional 5 min at 25 ℃ in the dark. Finally, the percentage of apoptotic cells was determined by BD FACSCanto™ II flow cytometry analysis (BD Biosciences, San Jose, CA, USA). Briefly, cells were first gated on forward scatter area (FSC-A) vs. side scatter area (SSC-A) to exclude debris, followed by single-cell gating using forward scatter height (FSC-H) vs. FSC-A. Then, within this gated population, cells were analyzed for Annexin V-FITC and PI staining. The quadrants were set using appropriate unstained and single-stained controls: Annexin V-negative/PI-negative cells (live cells), Annexin V-positive/PI-negative cells (early apoptotic), Annexin V-positive/PI-positive cells (late apoptotic/necrotic), and Annexin V-negative/PI-positive cells (necrotic or damaged). The percentage of apoptotic cells was determined as the sum of early apoptotic (Annexin V+/PI-) and late apoptotic (Annexin V+/PI+) populations, divided by the total number of gated cells, multiplied by 100. This calculation method is standard and was consistently applied across all experimental groups. The assay was repeated at least three times independently (biological replicates).

*2.9 Western Blotting*

Protein expression was assessed by preparing lysates from cells, tissues, or exosomes using radioimmunoprecipitation assay (RIPA) buffer (Beyotime) containing protease inhibitors. Following separation by SDS–PAGE, proteins were transferred onto polyvinylidene difluoride (PVDF) (ISEQ00010, Millipore, Merck, Germany) membranes. The membranes were blocked with 5% bovine serum albumin (BSA) (ST023, Beyotime) and subsequently probed with primary antibodies. Chemiluminescent signals were detected using a Tanon 5200 imaging system (Tanon, Shanghai, China) after incubation with horseradish peroxidase-conjugated secondary antibodies. The protein expression was quantified and normalized to that of actin. Quantification was performed on data from three independent biological replicates (n = 3) by a researcher blinded to the experimental groups.

*2.10 Immunofluorescence Staining*

Post-treatment, cells on coverslips or brain slices were incubated overnight at 4 °C with primary antibodies, washed with 1× PBS, and then incubated with fluorescent-labeled secondary antibodies. Afterward, cell nuclei were counterstained with DAPI. Images were captured using an LSM 980 confocal laser-scanning microscope (Carl Zeiss Microscopy GmbH, Jena, Germany). Quantitative analysis of fluorescence intensity was conducted using Image-Pro Plus 8.0 software (Media Cybernetics, Bethesda, MD, USA). Specifically, first, all samples were processed in parallel using the same batch of reagents, and fluorescence staining was performed simultaneously under identical conditions. Second, we included internal controls (e.g., untreated cells) on each experimental plate to normalize signal intensities. Third, imaging parameters (exposure time, gain, laser power) were kept constant for all samples within a given experiment, and we used automated image acquisition to minimize operator-induced variability. Additionally, we performed background subtraction and used fluorescence intensity normalization relative to a housekeeping protein or cellular marker (e.g., DAPI for nuclear staining) to account for cell number or seeding density differences. Finally, statistical analysis was applied to ensure observed differences were reproducible and significant. Each experiment was assessed through three independent replicates.

*2.11 Statistical Analysis*

Statistical analyses were performed using GraphPad Prism 8.0 (GraphPad Software Inc., San Diego, CA, USA). Data were obtained from three independent experiments and presented as mean ± standard deviation (SD). Statistical significance was calculated based on one-way ANOVA. For multiple comparisons, we applied the Bonferroni correction to control for family-wise error rates. $p$ value $< 0.05$ was considered statistically significant.

## 3. Results

### *3.1 Identification and Bioinformatics Analysis of the Serum Cytokines in the PD Mouse Model Treated With T-MSCs*

Our previous study used commercial embryonic stem cells to obtain special mesenchymal-like stem cells, namely T-MSCs, at the trophoblast stage, which showed the characteristics of multipotent mesenchymal stem cells [35]. T-MSCs could improve the motor behavior disorder of PD mice, alleviate α-syn aggregation, and repair damaged DA neurons. Accumulating evidence implicates chronic central and peripheral immune–inflammatory mechanisms as contributing to PD pathogenesis, which may be reflected by alterations in circulating signaling protein concentrations [38,39]. We analyzed serum samples from the chronic PD mouse model using antibody arrays to screen for therapeutic proteins among 200 serum cytokines. Consequently, we identified 12 cytokines exhibiting statistically significant differences (Fig. 1A). Meanwhile, Gene Ontology (GO) classification revealed the involvement of apoptotic signaling pathway, which has been implicated in neurodegeneration, especially in PD (Fig. 1B). Subsequently, Kyoto Encyclopedia of Genes and Genomes (KEGG) pathway analysis was performed to reveal expression changes of functionally related cytokines (Fig. 1C). Following bioinformatics analysis, we validated the selected Clusterin through GSM-CAA-4000 using ELISA kits and found that the serum Clusterin levels in PD mice showed an increasing trend compared to those of the mice in the control group; however, the levels decreased after treatment with T-MSCs (Fig. 1D). This was consistent with the microarray analysis results. Notably, the cytokine Clusterin has been previously reported to be associated with apoptosis, especially in PD [40].

### *3.2 T-MSCs Decrease Apoptosis in MPTP-induced Models by Inhibiting the Caspase-8/Caspase-3 Pathway*

Apoptosis, also known as programmed cell death (PCD), is a fundamental physiological phenomenon of cell self-destruction, which is typically divided into caspase-dependent and non-caspase-dependent apoptosis. Caspase-8 and Caspase-3 are at the core of the caspase cascade reaction as initiator and executor, respectively. These are vital steps in cell apoptosis and the main pathways for signal transduction [41]. Meanwhile, to explore potential connections with exogenous Caspase-8 pathways, a study has shown that treatment with the specific Caspase-8 inhibitor (zIETD fmk) significantly reduced the observed apoptotic phenotype of cells, indicating that Caspase-8 inhibition has a protective effect [42]. Another study conducted in 2026 found that activation of Caspase-8 can participate in autophagy stimulation triggering through the PI3K/mTOR pathway, leading to apoptosis [43]. Combined with the established paradigm of its placement in the extrinsic pathway, this strongly supports focusing research on this mechanism.

It is widely known that MSCs primarily exert antiapoptotic effects in various organs by secreting diverse growth factors or inducing the transcription of mRNA or miRNA linked to cell proliferation. To further investigate the *in vitro* effects of T-MSCs, we utilized the MN9D murine neuronal cell line and employed a pre-determined concentration of $MPP^+$ (500 μM) to establish a cellular PD model. The FCM analysis of apoptosis revealed a significant increase in the apoptotic rate within the MN9D cell model. Concurrently, this rate was markedly reduced following T-MSCs treatment (Fig. 2A,B). Subsequently, we conducted a cellular-level investigation to determine whether T-MSCs enhance the anti-apoptotic capacity of $MPP^+$-induced MN9D cells by inhibiting the Caspase-8/Caspase-3 pathway. The western blotting results demonstrated that, relative to the control group, the expression of Caspase-8, Bax, and Cleaved caspase-3 in MN9D cells treated with $MPP^+$ increased, whereas the expression of antiapoptotic protein Bcl-2 decreased. However, compared with the $MPP^+$ group, the expression of Caspase-8, Bax, and Cleaved caspase-3 in the $MPP^+$ + T-MSCs group considerably decreased, alongside an increase in Bcl-2 expression (Fig. 2C–G, the original western blotting images can be found in the **Supplementary Material**). These observations suggest that T-MSCs enhance the anti-apoptotic potential of $MPP^+$-induced MN9D cells by suppressing the Caspase-8/Caspase-3 signaling pathway.

We subsequently examined whether PD mice exhibited an antiapoptotic effect comparable to that of T-MSCs. These findings aligned with our *in vitro* observations. The Western blotting assay showed reduced expression of Caspase-8, Bax, and Cleaved caspase-3 in T-MSCs-treated PD mice (Fig. 3, the original western blotting images can be found in the **Supplementary Material**) in the substantia nigra samples. These data indicate that T-MSCs intervention enhances the anti-apoptotic capacity in PD mice by upregulating Bcl-2 expression through inhibition of the Caspase-8/Caspase-3 pathway.

### *3.3 T-MSCs-sEVs Mitigate Apoptosis in PD by Inhibiting the Caspase-8/Caspase-3 Pathway, Akin to the Effects of T-MSCs*

Previously, we validated that T-MSCs can inhibit the apoptotic effect produced by $MPP^+$-induced MN9D cells. Further research is needed to determine whether T-MSCs-sEVs, a secretion of T-MSCs, can produce similar effects. In $MPP^+$-induced MN9D cells, the significantly increased apoptosis rate observed compared to controls was substantially reduced in the $MPP^+$ + T-MSCs-sEVs group relative to the $MPP^+$ group (Fig. 4A,C). The findings indicate that T-MSCs-sEVs can decrease apoptosis in MN9D cells induced by $MPP^+$.

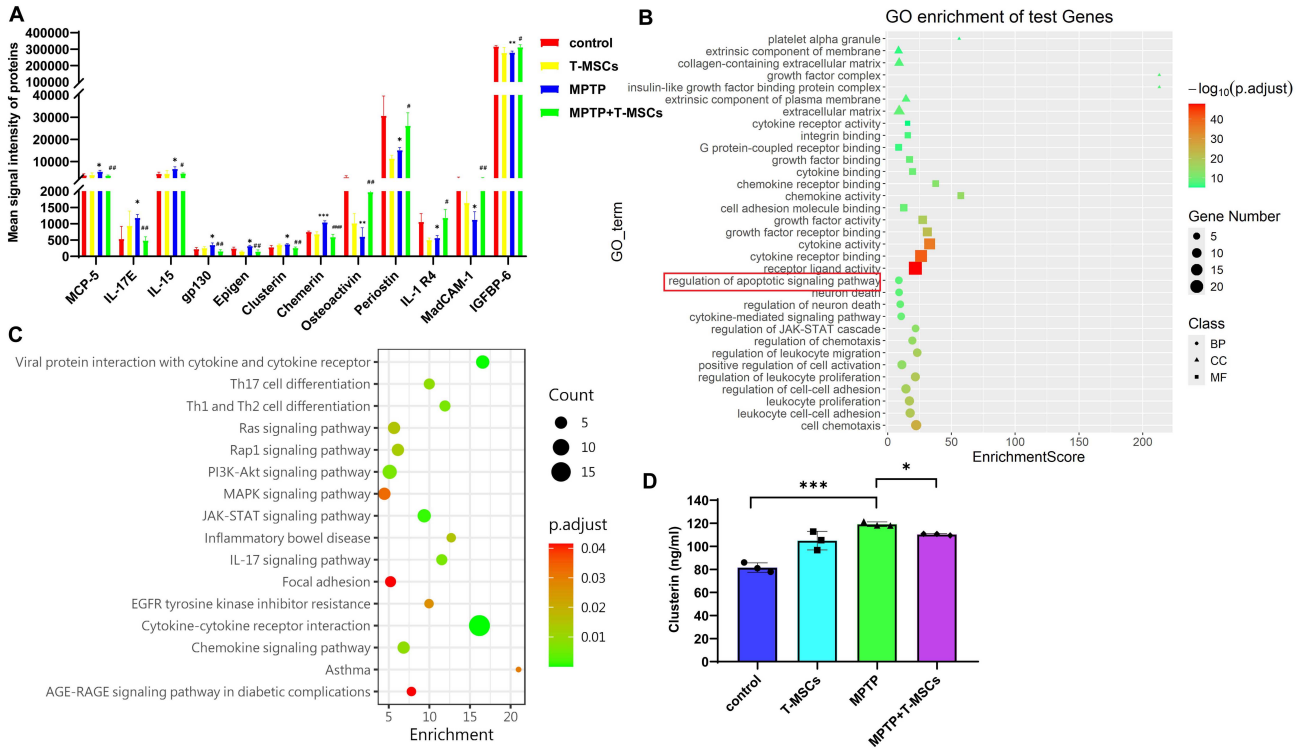


**Fig. 1. Identification and bioinformatics analysis of cytokines that may exert regulatory effects**. Serum samples were collected from a PD mouse model and screened for potential therapeutic proteins using the GSM-CAA-4000 array targeting 200 serum cytokines. (A) Serum cytokines of T-MSCs treatment in control or MPTP-induced PD mice (n = 3 per group) were measured by the antibody array test. Normalized signal values were analyzed by one-way ANOVA, and signal values >100 are listed. Control group vs. MPTP group, *$p < 0.05$, **$p < 0.01$, ***$p < 0.001$; MPTP + T-MSCs group vs. MPTP group, #$p < 0.05$, ##$p < 0.01$, ####$p < 0.0001$. (B) GO analysis, including three subtypes: BP (biological process), MF (molecular function), and CC (cellular component). (C) KEGG analysis. (D) Serum Clusterin expression was verified by ELISA (n = 3 per group). Experiments were performed in triplicate. Data are presented as the mean ± SD. One-way ANOVA was used to analyze the data. *$p < 0.05$, ***$p < 0.001$. PD, Parkinson's disease; T-MSCs, trophoblast-derived mesenchymal-like stem cells; KEGG, Kyoto Encyclopedia of Genes and Genomes; SD, standard deviation; MPTP, 1-Methyl-4-phenyl-1,2,3,6-tetrahydropyridine hydrochloride; GO, Gene Ontology; BP, biological process; MF, molecular function; CC, cellular component.

Next, we investigated whether T-MSCs-sEVs could upregulate Bcl-2 expression through the Caspase-8/Caspase-3 pathway *in vitro*. In contrast to the $MPP^+$ group, the $MPP^+$ + T-MSCs-sEVs group exhibited decreased expression of Caspase-8 and Bax, alongside an increase in Bcl-2 expression (Fig. 4E–H, the original western blotting images can be found in the **Supplementary Material**). Concurrently, a significant decrease in fluorescence intensity of Caspase-3, a pro-apoptotic protein, was observed under T-MSCs-sEVs treatment (Fig. 4B,D). The data indicate that T-MSCs likely enhance Bcl-2 expression by secreting T-MSCs-sEVs, thereby inhibiting the Caspase-8/Caspase-3 pathway and increasing the antiapoptotic capacity of MN9D cells.

Previous research has established that T-MSCs-sEVs can cross the BBB and selectively target DA neurons in the SNpc, indicating their potential utility as a delivery vehicle for therapeutic compounds [35]. We subsequently analyzed whether T-MSCs-sEVs exhibited a comparable antiapoptotic effect in PD mice. The outcomes aligned with our prior *in vitro* findings. Western blotting indicated that the pro-apoptotic proteins (including Caspase-8, Bax, and Cleaved caspase-3) had decreased expression, alongside an upregulation of the antiapoptotic protein Bcl-2 following T-MSCs-sEVs treatment from the substantia nigra samples (Fig. 5, the original western blotting images can be found in the **Supplementary Material**). Overall, T-MSCs-sEVs, secreted by T-MSCs, contribute to PD models protection and exhibit antiapoptotic effects by inhibiting the Caspase-8/Caspase-3 pathway.

In conclusion, intravenous injection of T-MSCs and T-MSCs-sEVs showed therapeutic potential in PD models. Antibody microarray analysis revealed that T-MSCs treatment elevated serum clusterin levels, which were associated with apoptosis, particularly in PD. In addition, T-MSCs-sEVs, derived from T-MSCs, enhanced the antiapoptotic effects of DA neurons by promoting neuronal repair by inhibiting the Caspase-8/Caspase-3 pathway.

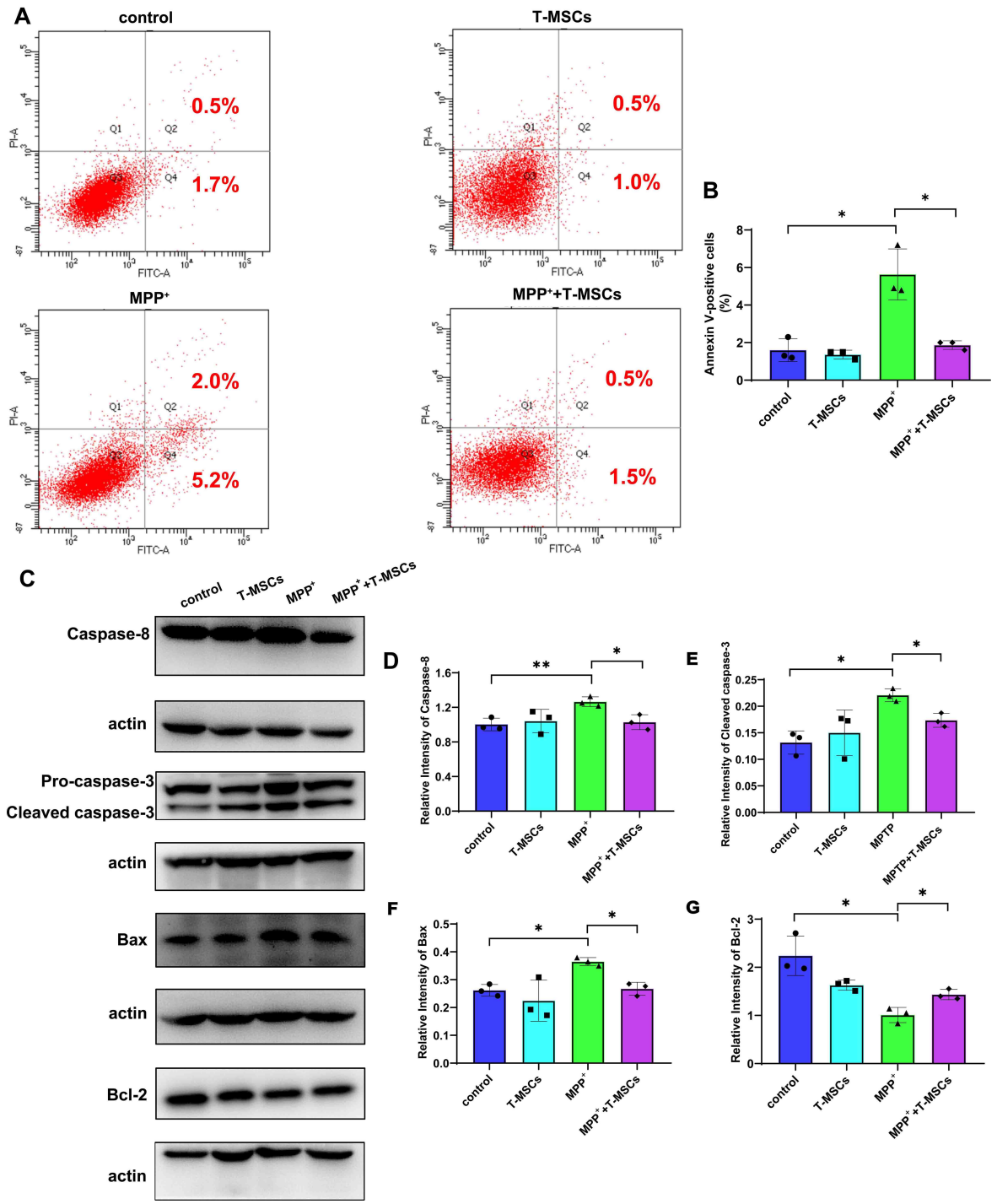


**Fig. 2. T-MSCs enhanced the antiapoptotic ability of MPP$^+$-induced MN9D cells by inhibiting the Caspase-8/Caspase-3 pathway**. T-MSCs and MN9D cells were co-cultured for 24 h using a Transwell system. Subsequently, MN9D cells were treated with 500 μM MPP$^+$ and co-cultured for an additional 24 h. The experimental design comprised four groups: a control group, T-MSCs group, MPP$^+$ group, and MPP$^+$ + T-MSCs group. (A,B) Flow cytometric analysis of the apoptosis rate upon T-MSCs treatment in control or MPP$^+$-induced MN9D cells. Representative flow cytometry plots from one experiment are shown in (A); quantification of total apoptosis (early + late) from three independent experiments is presented in (B) as mean ± SD. (C) Western blotting assay for Caspase-8, Pro-caspase-3, Cleaved caspase-3, Bax, and Bcl-2 expression in cell lysates. (D–G) Quantitative statistical analysis of the grey-scale values of the bands for Caspase-8, Cleaved caspase-3, Bax, and Bcl-2, respectively. Experiments were performed in triplicate. The results are shown as the mean ± SD. One-way ANOVA was used to analyze the data. *$p < 0.05$, **$p < 0.01$.

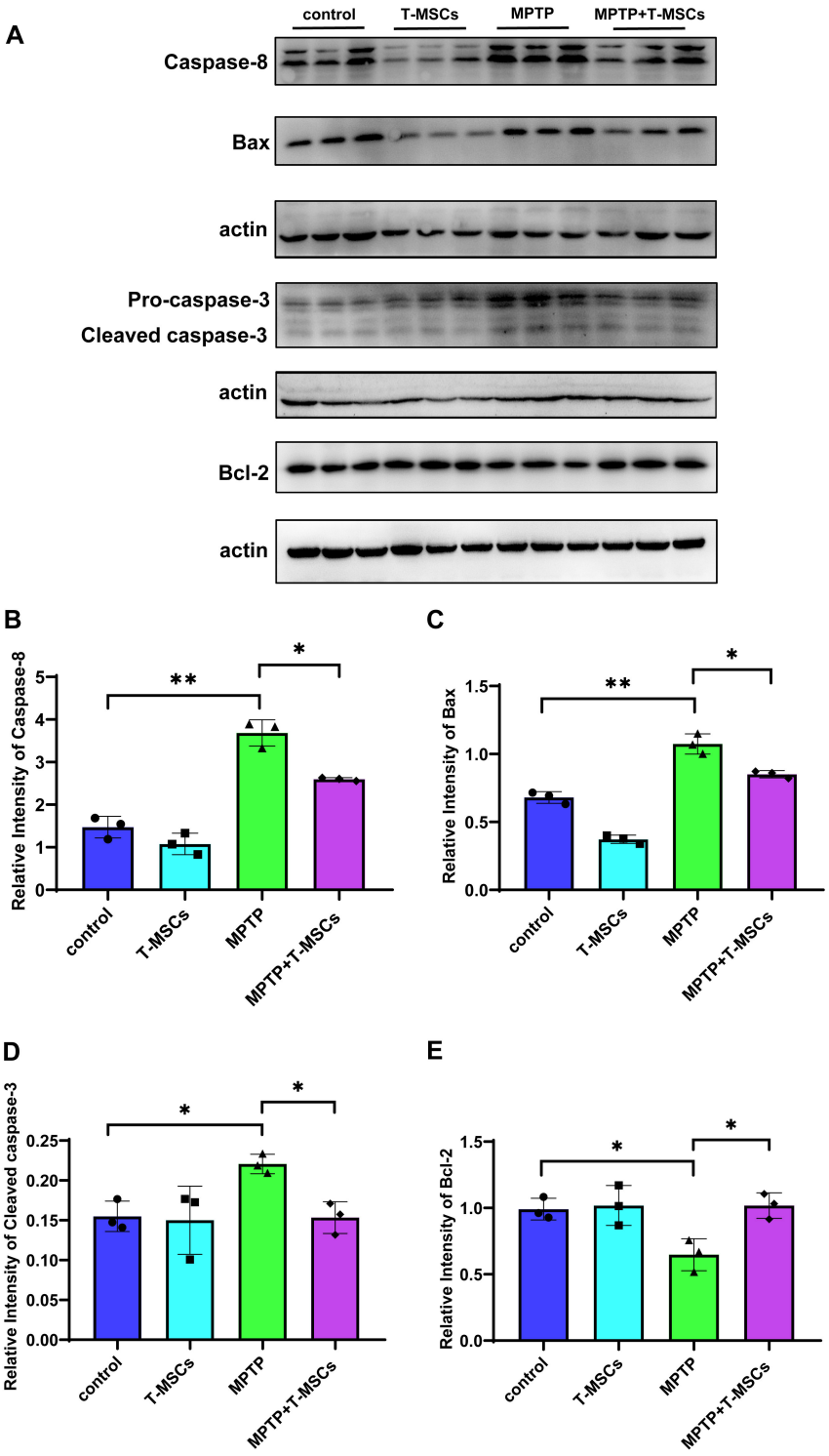


**Fig. 3. T-MSCs inhibit apoptosis in a PD mouse model through the Caspase-8/Caspase-3 pathway**. Chronic PD mouse model was developed using MPTP, administered intraperitoneally at 25 mg/kg twice weekly for 5 weeks. T-MSCs were administered via the intravenous injection (i.v.) on days 3, 17, and 31 after the start of the modeling (cell count $5 \times 10^5$/100 µL PBS). The study included four groups: the control group, T-MSCs group, MPTP group, and MPTP + T-MSCs group. (A) Representative blots showed the levels of Caspase-8, Cleaved caspase-3, Bax, and Bcl-2. (B–E) Quantitative statistical analysis of the grey-scale values of the bands for Caspase-8, Bax, Cleaved caspase-3, and Bcl-2, respectively. n = 3 per group. The results are presented as the mean ± SD. The data were analyzed using one-way ANOVA. *$p < 0.05$, **$p < 0.01$.

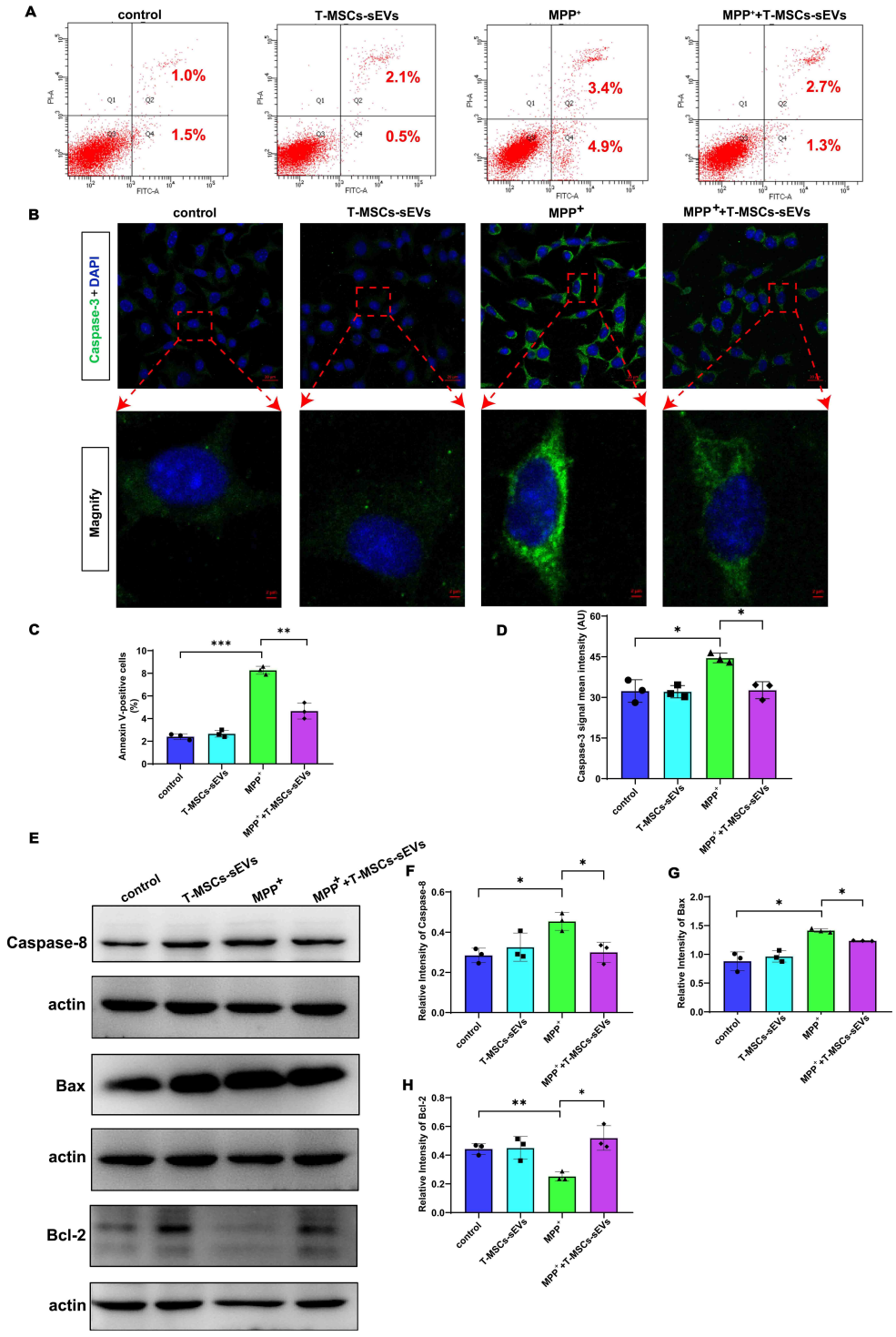


**Fig. 4. T-MSCs-sEVs inhibit apoptosis in MPP$^+$-induced MN9D cells via the Caspase-8/Caspase-3 pathway**. MN9D cells were seeded into 6-well plates. The experiment was divided into four groups: the control group, T-MSCs-sEVs group, MPP$^+$ group, and MPP$^+$ + T-MSCs-sEVs group. Three replicate wells were set up for each group. Cells were treated with medium, MPP$^+$, or T-MSCs-sEVs. After 24 h of MPP$^+$ (500-μM concentration) treatment, T-MSCs-sEVs were added for 24 h. (A,C) Flow cytometry analysis of the apoptosis rate upon T-MSCs-sEVs treatment in the control or MPP$^+$-induced MN9D cells. (B,D) Immunofluorescent staining and quantification of Caspase-3 in the control, T-MSCs-sEVs, MPP$^+$, and MPP$^+$ + T-MSCs-sEVs groups. Scale bars: upper, 20 μm; lower, 2 μm. (E–H) Western blotting analysis of Caspase-8, Bax, and Bcl-2 expression upon T-MSCs-sEVs treatment in the control or MPP$^+$-induced MN9D cells. Experiments were performed in triplicate. Data are presented as mean ± SD. Statistical analysis was performed using one-way ANOVA. *$p < 0.05$, **$p < 0.01$, ***$p < 0.001$. T-MSCs-sEVs, small extracellular vesicles secreted by T-MSCs.

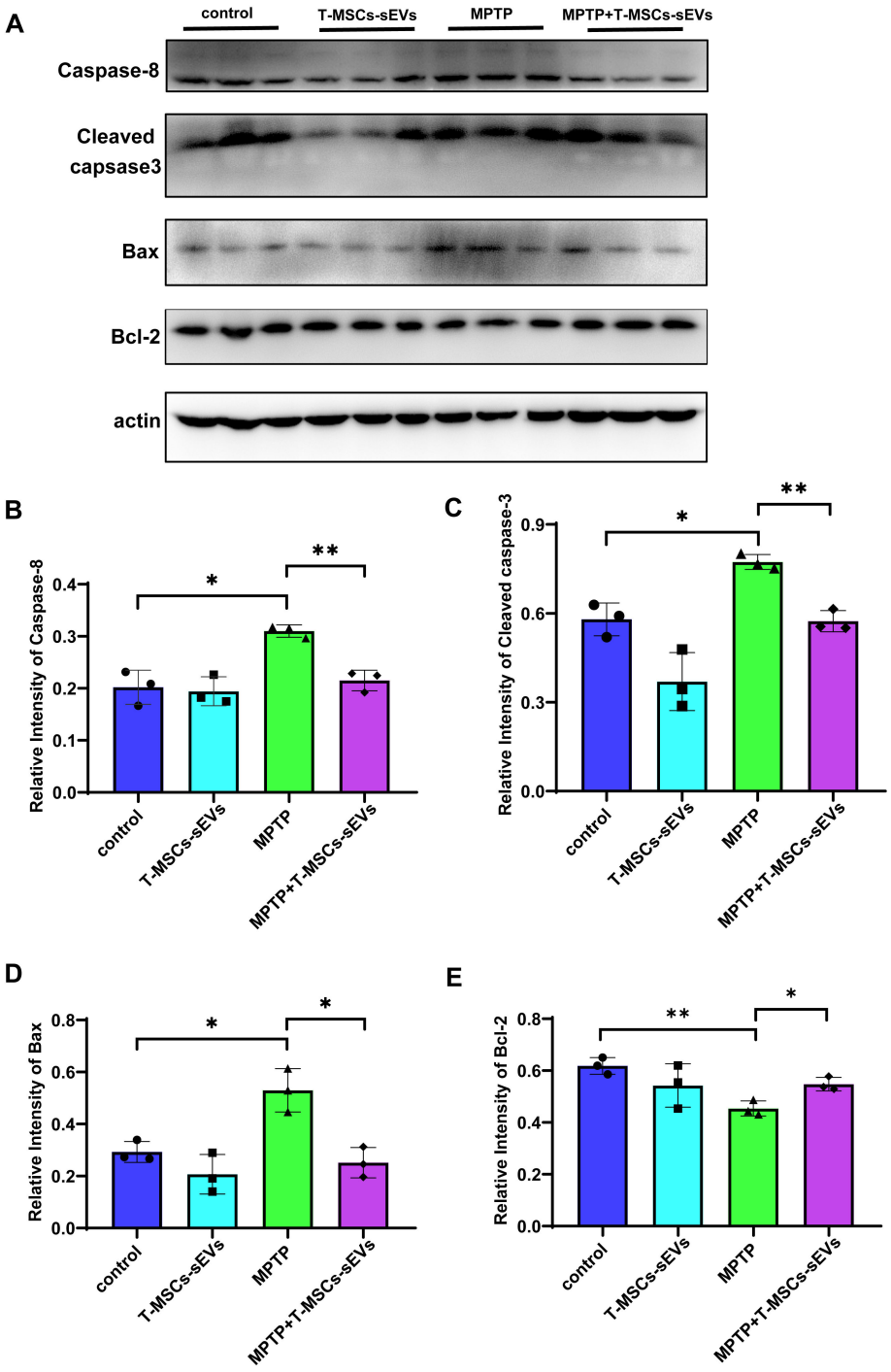


**Fig. 5. T-MSCs-sEVs inhibit apoptosis in a PD mouse model through the Caspase-8/Caspase-3 pathway**. Chronic PD mouse model was established using MPTP (intraperitoneal injection, 25 mg/kg, twice weekly for five weeks). T-MSCs-sEVs were given in the tail vein on day 3, 17, and 31 after the start of the modeling ($7.32 \times 10^{10}$ particles/mL). The study included four groups: a control group, T-MSCs-sEVs group, MPTP group, and MPTP + T-MSCs-sEVs group. (A) Representative blots showing the levels of Caspase-8, Cleaved caspase-3, Bax, and Bcl-2. (B–E) Quantitative statistical analysis of the grey-scale values of the bands for Caspase-8, Cleaved caspase-3, Bax, and Bcl-2, respectively. n = 3 per group. The results are shown as the mean ± SD. One-way ANOVA was used to analyze the data. *$p < 0.05$, **$p < 0.01$.

## 4. Discussion

PD is the second most common neurodegenerative disorder after Alzheimer's disease (AD), posing a substantial burden on healthcare systems worldwide [44,45]. The neuropathological feature of PD is the selective loss of DA neurons in the SNpc, which leads to a decrease in striatal

DA and the formation of α-syn [46,47,48]. PD has a slow onset and a long course, and the main clinical feature is movement disorders. Furthermore, patients with advanced PD face a severely reduced quality of life, resulting in a heavy burden on their families and society [5,49,50]. At present, disease-modifying therapies for PD are still lacking. Therefore, it has become imperative to develop effective targeting drugs for patients with PD.

Although MSCs have been used in disease treatment, their source is relatively difficult, which can be efficiently generated from embryonic stem cells via a trophoblast intermediate within 11–16 days [35]. After library screening, embryonic stem cells can differentiate into therapeutic MSCs. Moreover, we previously clarified that T-MSCs and their secreted T-MSCs-sEVs can enhance the antioxidant capacity of PD models by activating the Keap1-Nrf2-SOD pathway [35]. Based on that prior research, we have continued to explore whether T-MSCs can exert other protective effects against PD models through small extracellular vesicles, such as antiapoptotic effects.

In this study, we established a chronic PD mouse model and administered T-MSCs to identify potential therapeutic proteins. Using antibody arrays targeting 200 serum cytokines, we identified Clusterin as a cytokine associated with apoptosis (Fig. 1). There is a certain discrepancy with what was previously reported by Zhu et al. [40], which indicated that secretory clusterin (sCLU) could decrease the Bax/Bcl-2 ratio and the Cleaved caspase-3 expression in the SN of MPTP-induced PD mice. In our PD models, the initial elevated levels of Clusterin likely represent a stress-induced, compensatory response to cellular injury. The subsequent reduction in Clusterin after T-MSCs treatment does not negate its protective function but rather suggests that the therapeutic intervention mitigated the initial injury signal, thereby reducing the need for this compensatory response. To further explore the specific molecular mechanisms, we investigated the related apoptotic proteins. Combined with the FCM assay results, we confirmed that T-MSCs could effectively inhibit MN9D cell apoptosis (Fig. 2A,B). Moreover, through *in vivo* and *in vitro* experiments, we verified that T-MSCs could upregulate the expression of the antiapoptotic protein Bcl-2 by inhibiting the Caspase-8/Caspase-3 pathway (Fig. 2C–G and Fig. 3). This is in agreement with the results of Gu et al. [51], who demonstrated that endogenous IL-6 of MSCs could have the potential therapeutic effects against a hypoxic-ischemic brain damage neonatal rat model mainly through the IL-6/STAT3 signaling pathway. Meanwhile, Huang et al. [52] also reported that hPSC-derived ectomesenchymal stromal cells mitigated hypoxic–ischemic brain damage by promoting antiapoptotic effects, neurite outgrowth, and neurogenesis through the ERK/CREB pathway. Furthermore, other reports have shown that neurotrophic factor-primed mesenchymal stromal cells suppressed the induction of apoptotic markers *Bax* and *Sirt1*, considerably restoring ER stress-induced loss of neuro-regenesis [53]. Overall, our study indicates that T-MSCs contribute to the protection of PD models through the Caspase-8/Caspase-3 pathway, offering a solid foundation for future research.

It is unclear whether T-MSCs-sEVs, which is produced by T-MSC secretion, could perform a similar function. According to a previous study, astrocyte-derived exosomal miR-200a-3p inhibits $MPP^+$-induced apoptosis by downregulating MKK4 [54]. Meanwhile, Luo et al. [55] demonstrated that epicatechin gallate encapsulated by bovine milk-derived exosomes (ECG-Exo) could have the potential therapeutic effects against a rotenone-induced PD SH-SY5Y cells mainly through antiapoptosis and antimitophagy. Furthermore, another study has demonstrated that curcumin-loaded human endometrial stem cell-derived exosomes can rescue 6-OHDA-induced neuronal apoptosis by increasing the antiapoptotic protein Bcl-2 expression level and reducing the expression of apoptosis markers Bax and Caspase-3 [56]. In our study, the antiapoptotic effect of T-MSCs-sEVs was well established by the FCM assay, similar to that of T-MSCs. In addition, *in vivo* and *ex vivo* experiments further validated that T-MSCs-sEVs, secreted by T-MSCs, suggest a potential neuroprotective role in the context of DA neuron survival through the Caspase-8/Caspase-3 pathway. These findings indicate that T-MSCs-sEVs effectively ameliorate DA neuron degeneration in PD models, aligning with our expectations.

In our study, we found that both T-MSCs and T-MSCs-sEVs contributed to the protective effects against PD models and demonstrated antiapoptotic properties by inhibiting the Caspase-8/Caspase-3 pathway. Nevertheless, several limitations of this study should be mentioned. First, our findings demonstrate the therapeutic potential of T-MSCs-sEVs as a separate treatment modality, but further studies with direct, dose-matched comparisons are needed to rigorously establish T-MSCs-sEVs as a cell-free alternative. Second, it is important to recognize the possible limitations of animal and cell models, which due to inherent species differences, may not perfectly replicate human diseases. Third, this study did not conduct a comprehensive investigation into critical parameters such as optimal treatment frequency, intensity, duration, and long-term safety. In addition, behavioral experiments should include baseline locomotion assessments prior to modeling or treatment to rule out non-specific activity changes unrelated to nigrostriatal protection. Furthermore, The study predominantly focused on the Caspase-8/Caspase-3 axis, but the pathogenic mechanism of PD is extensive and complex. Thus, future in-depth studies will be needed to examine these issues in more detail.

To overcome these aforementioned limitations, further studies will be devoted to proteomics and RNA sequencing (including lncRNA, miRNA, and circRNA) analysis of T-MSCs-sEVs to investigate the involvement of specific proteins or molecules in antiapoptotic regulation, fur-

ther clarifying the protective mechanism of PD from a microscopic perspective. Moreover, the metabolism of T-MSCs-sEVs will be monitored *in vivo* to explore its duration in PD treatment so as to better evaluate its safety and efficacy.

## 5. Conclusions

PD is a complex, multi-system neurodegenerative disorder. It is marked by the aggregation of α-syn and the degeneration of DA neurons in SNpc. This condition often results in significant disability and contributes to the growing global health burden through its motor, non-motor, and cognitive manifestations [57,58,59]. Consequently, there is a critical need to develop novel therapeutic agents and approaches that can decelerate or arrest disease progression. This research highlights the therapeutic promise of T-MSCs and T-MSCs-sEVs in enhancing antiapoptotic mechanisms in PD models by suppressing the Caspase-8/Caspase-3 signaling pathway. Although these findings are encouraging, more extensive, rigorously designed, and long-term studies are necessary to further elucidate the underlying pathological mechanisms of PD.

## Availability of Data and Materials

All data from this study can be obtained from the corresponding author upon reasonable request.

## Author Contributions

SQ: Conceptualization, Project administration, Data curation, Writing - review & editing, and Funding acquisition. SH: Investigation, Data curation, and Writing - original draft. QQ and YO: Data curation. LH, YY, and QW: Investigation. XW: Participated in the purification and identification of T-MSCs and T-MSCs-sEVs, and provided experimental data. All authors contributed to editorial changes in the manuscript. All authors read and approved the final manuscript. All authors have participated sufficiently in the work and agreed to be accountable for all aspects of the work.

## Ethics Approval and Consent to Participate

All experiments were conducted following the criteria outlined in the Guide for the Care and Use of Laboratory Animals and were approved by the Institutional Animal Care and Use Committee of Southern Medical University (NO. IACUC-LAC-20220606-009).


## Acknowledgment

Not applicable.

## Funding

This work was supported by grants from the National Natural Science Foundation of China (grant nos. U1603281 and 81870991 to SQ), the Jiangxi Provincial Natural Science Foundation (grant no. 20232ACB206021 to SQ), the Science and Technology Projects in Guangzhou (grant no. 2024B03J1257 to SQ), and the Science and Technology Planning Project of Ganzhou (grant no. GZ2024YLJ011).


## Conflicts of Interest

Xiaofang Wang holds positions at both the U.S. headquarters and the Chinese branch of ImStem Biotechnology Co., Ltd. All other authors have reported no conflicts relevant to the contents of this paper to disclose.

## Supplementary Material

Supplementary material associated with this article can be found, in the online version, at https://doi.org/10.31083/JIN49659.

## References


[1] Liu J, Liu W, Yang H. Balancing Apoptosis and Autophagy for Parkinson's Disease Therapy: Targeting BCL-2. ACS Chemical Neuroscience. 2019; 10: 792–802. https://doi.org/10.1021/acschemneuro.8b00356

[2] Al-Kuraishy HM, Al-Gareeb AI, Zaidalkiani AT, Alexiou A, Papadakis M, Bahaa MM, et al. Calprotectin in Parkinsonian disease: Anticipation and dedication. Ageing Research Reviews. 2024; 93: 102143. https://doi.org/10.1016/j.arr.2023.102143

[3] Xu L, Wang Z, Li Q. Global trends and projections of Parkinson's disease incidence: a 30-year analysis using GBD 2021 data. Journal of Neurology. 2025; 272: 286. https://doi.org/10.1007/s00415-025-13030-2

[4] Berg D, Postuma RB, Bloem B, Chan P, Dubois B, Gasser T, et al. Time to redefine PD? Introductory statement of the MDS Task Force on the definition of Parkinson's disease. Movement Disorders : Official Journal of the Movement Disorder Society. 2014; 29: 454–462. https://doi.org/10.1002/mds.25844

[5] Ben-Shlomo Y, Darweesh S, Llibre-Guerra J, Marras C, San Luciano M, Tanner C. The epidemiology of Parkinson's disease. Lancet (London, England). 2024; 403: 283–292. https://doi.org/10.1016/S0140-6736(23)01419-8

[6] GBD 2016 Parkinson's Disease Collaborators. Global, regional, and national burden of Parkinson's disease, 1990-2016: a systematic analysis for the Global Burden of Disease Study 2016. The Lancet. Neurology. 2018; 17: 939–953. https://doi.org/10.1016/S1474-4422(18)30295-3

[7] Bloem BR, Okun MS, Klein C. Parkinson's disease. Lancet (London, England). 2021; 397: 2284–2303. https://doi.org/10.1016/S0140-6736(21)00218-X

[8] Ho HY, Chen PJ, Chuang YC, Lo YS, Lin CC, Hsieh MJ, et al. Picrasidine I Triggers Heme Oxygenase-1-Induced Apoptosis in Nasopharyngeal Carcinoma Cells via ERK and Akt Signaling Pathways. International Journal of Molecular Sciences. 2022; 23: 6103. https://doi.org/10.3390/ijms23116103

[9] Zhang Q, Riley-Gillis B, Han L, Jia Y, Lodi A, Zhang H, et al. Activation of RAS/MAPK pathway confers MCL-1 mediated acquired resistance to BCL-2 inhibitor venetoclax in acute myeloid leukemia. Signal Transduction and Targeted Therapy. 2022; 7: 51. https://doi.org/10.1038/s41392-021-00870-3

[10] André S, Picard M, Cezar R, Roux-Dalvai F, Alleaume-Butaux A, Soundaramourty C, et al. T cell apoptosis characterizes severe Covid-19 disease. Cell Death and Differentiation. 2022; 29: 1486–1499. https://doi.org/10.1038/s41418-022-00936-x

[11] Carter BZ, Mak PY, Tao W, Ayoub E, Ostermann LB, Huang X, et al. Combined inhibition of BCL-2 and MCL-1 overcomes

BAX deficiency-mediated resistance of TP53-mutant acute myeloid leukemia to individual BH3 mimetics [published erratum in Blood Cancer Journal. 2023; 13: 80]. Blood Cancer Journal. 2023; 13: 57. https://doi.org/10.1038/s41408-023-00830-w

[12] Czabotar PE, Garcia-Saez AJ. Mechanisms of BCL-2 family proteins in mitochondrial apoptosis. Nature Reviews. Molecular Cell Biology. 2023; 24: 732–748. https://doi.org/10.1038/s41580-023-00629-4

[13] Kumar S, Budhathoki S, Oliveira CB, Kahle AD, Calhan OY, Lukens JR, et al. Role of the caspase-8/RIPK3 axis in Alzheimer's disease pathogenesis and Aβ-induced NLRP3 inflammasome activation. JCI Insight. 2023; 8: e157433. https://doi.org/10.1172/jci.insight.157433

[14] Huang YP, Hsia TC, Yeh CA, Ma YS, Hsu SY, Liu YC, et al. PW06 Triggered Fas-FADD to Induce Apoptotic Cell Death In Human Pancreatic Carcinoma MIA PaCa-2 Cells through the Activation of the Caspase-Mediated Pathway. Oxidative Medicine and Cellular Longevity. 2023; 2023: 3479688. https://doi.org/10.1155/2023/3479688

[15] Mahul-Mellier AL, Burtscher J, Maharjan N, Weerens L, Croisier M, Kuttler F, et al. The process of Lewy body formation, rather than simply α-synuclein fibrillization, is one of the major drivers of neurodegeneration. Proceedings of the National Academy of Sciences of the United States of America. 2020; 117: 4971–4982. https://doi.org/10.1073/pnas.1913904117

[16] Zheng Z, Zhang S, Zhang H, Gao Z, Wang X, Liu X, et al. Mechanisms of Autoimmune Cell in DA Neuron Apoptosis of Parkinson's Disease: Recent Advancement. Oxidative Medicine and Cellular Longevity. 2022; 2022: 7965433. https://doi.org/10.1155/2022/7965433

[17] Mehra S, Sahay S, Maji SK. α-Synuclein misfolding and aggregation: Implications in Parkinson's disease pathogenesis. Biochimica et Biophysica Acta. Proteins and Proteomics. 2019; 1867: 890–908. https://doi.org/10.1016/j.bbapap.2019.03.001

[18] Pan Y, Zong Q, Li G, Wu Z, Du T, Huang Z, et al. Nuclear localization of alpha-synuclein affects the cognitive and motor behavior of mice by inducing DNA damage and abnormal cell cycle of hippocampal neurons. Frontiers in Molecular Neuroscience. 2022; 15: 1015881. https://doi.org/10.3389/fnmol.2022.1015881

[19] Lin D, Zhang H, Zhang J, Huang K, Chen Y, Jing X, et al. α-Synuclein Induces Neuroinflammation Injury through the IL6ST-AS/STAT3/HIF-1α Axis. International Journal of Molecular Sciences. 2023; 24: 1436. https://doi.org/10.3390/ijms24021436

[20] Jia X, Chen Q, Yao C, Asakawa T, Zhang Y. α-synuclein regulates Cyclin D1 to promote abnormal initiation of the cell cycle and induce apoptosis in dopamine neurons. Biomedicine & Pharmacotherapy = Biomedecine & Pharmacotherapie. 2024; 173: 116444. https://doi.org/10.1016/j.biopha.2024.116444

[21] He S, Chen Y, Wang H, Li S, Wei Y, Zhang H, et al. Neuroprotective effects of chlorogenic acid: Modulation of Akt/Erk1/2 signaling to prevent neuronal apoptosis in Parkinson's disease. Free Radical Biology & Medicine. 2024; 222: 275–287. https://doi.org/10.1016/j.freeradbiomed.2024.06.018

[22] Ray B, Tuladhar S, Nagaraju PG, Shivalinga A, Mahalakshmi AM, Priyadarshini P, et al. Telmisartan Protects Mitochondrial Function, Gait, and Neuronal Apoptosis by Activating the Akt/GSK3β/PGC1α Pathway in an MPTP-Induced Mouse Model of Parkinson's Disease. Journal of Integrative Neuroscience. 2024; 23: 29. https://doi.org/10.31083/j.jin2302029

[23] Meng T, Zhang Y, Huang J, Pandey V, Fu S, Ma S. Rubusoside mitigates neuroinflammation and cellular apoptosis in Parkinson's disease, and alters gut microbiota and metabolite composition. Phytomedicine : International Journal of Phytotherapy and Phytopharmacology. 2024; 124: 155309. https://doi.org/10.1016/j.phymed.2023.155309

[24] Shepherd CE, Affleck AJ, Bahar AY, Carew-Jones F, Halliday GM. Intracellular and secreted forms of clusterin are elevated early in Alzheimer's disease and associate with both Aβ and tau pathology. Neurobiology of Aging. 2020; 89: 129–131. https://doi.org/10.1016/j.neurobiolaging.2019.10.025

[25] Du X, Chen Z, Shui W. Clusterin: structure, function and roles in disease. International Journal of Medical Sciences. 2025; 22: 887–896. https://doi.org/10.7150/ijms.107159

[26] Mao L, Yin R, Yang L, Zhao D. Elucidating the function of clusterin in the progression of diabetic kidney disease. Frontiers in Pharmacology. 2025; 16: 1573654. https://doi.org/10.3389/fphar.2025.1573654

[27] Sultana P, Novotny J. Clusterin: a double-edged sword in cancer and neurological disorders. EXCLI Journal. 2024; 23: 912–936. https://doi.org/10.17179/excli2024-7369

[28] Přikrylová Vranová H, Hényková E, Mareš J, Kaiserová M, Menšíková K, Vaštík M, et al. Clusterin CSF levels in differential diagnosis of neurodegenerative disorders. Journal of the Neurological Sciences. 2016; 361: 117–121. https://doi.org/10.1016/j.jns.2015.12.023

[29] Zou J, Yang W, Cui W, Li C, Ma C, Ji X, et al. Therapeutic potential and mechanisms of mesenchymal stem cell-derived exosomes as bioactive materials in tendon-bone healing. Journal of Nanobiotechnology. 2023; 21: 14. https://doi.org/10.1186/s12951-023-01778-6

[30] Zheng J, Lu Y, Lin Y, Si S, Guo B, Zhao X, et al. Epitranscriptomic modifications in mesenchymal stem cell differentiation: advances, mechanistic insights, and beyond. Cell Death and Differentiation. 2024; 31: 9–27. https://doi.org/10.1038/s41418-023-01238-6

[31] Mei R, Wan Z, Yang C, Shen X, Wang R, Zhang H, et al. Advances and clinical challenges of mesenchymal stem cell therapy. Frontiers in Immunology. 2024; 15: 1421854. https://doi.org/10.3389/fimmu.2024.1421854

[32] Chen HX, Liang FC, Gu P, Xu BL, Xu HJ, Wang WT, et al. Exosomes derived from mesenchymal stem cells repair a Parkinson's disease model by inducing autophagy. Cell Death & Disease. 2020; 11: 288. https://doi.org/10.1038/s41419-020-2473-5

[33] Chen WST, Lin TY, Kuo CH, Hsieh DJY, Kuo WW, Liao SC, et al. Ginkgolide A improves the pleiotropic function and reinforces the neuroprotective effects by mesenchymal stem cell-derived exosomes in 6-OHDA-induced cell model of Parkinson's disease. Aging. 2023; 15: 1358–1370. https://doi.org/10.18632/aging.204526

[34] Wang CC, Hu XM, Long YF, Huang HR, He Y, Xu ZR, et al. Treatment of Parkinson's disease model with human umbilical cord mesenchymal stem cell-derived exosomes loaded with BDNF. Life Sciences. 2024; 356: 123014. https://doi.org/10.1016/j.lfs.2024.123014

[35] He S, Wang Q, Chen L, He YJ, Wang X, Qu S. miR-100a-5p-enriched exosomes derived from mesenchymal stem cells enhance the anti-oxidant effect in a Parkinson's disease model via regulation of Nox4/ROS/Nrf2 signaling. Journal of Translational Medicine. 2023; 21: 747. https://doi.org/10.1186/s12967-023-04638-x

[36] Wang X, Sun G, Feng T, Zhang J, Huang X, Wang T, et al. Sodium oligomannate therapeutically remodels gut microbiota and suppresses gut bacterial amino acids-shaped neuroinflammation to inhibit Alzheimer's disease progression. Cell Research. 2019; 29: 787–803. https://doi.org/10.1038/s41422-019-0216-x

[37] Huang P, Wan Z, Qu S. Targeting the RUNX3-miR-186-3p-DAT-IGF1R axis as a therapeutic strategy in a Parkinson's disease model. Journal of Translational Medicine. 2024; 22: 719.

https://doi.org/10.1186/s12967-024-05535-7
[38] Mahlknecht P, Stemberger S, Sprenger F, Rainer J, Hametner E, Kirchmair R, et al. An antibody microarray analysis of serum cytokines in neurodegenerative Parkinsonian syndromes. Proteome Science. 2012; 10: 71. https://doi.org/10.1186/1477-5956-10-71
[39] Walker DG, Lue LF, Serrano G, Adler CH, Caviness JN, Sue LI, et al. Altered Expression Patterns of Inflammation-Associated and Trophic Molecules in Substantia Nigra and Striatum Brain Samples from Parkinson's Disease, Incidental Lewy Body Disease and Normal Control Cases. Frontiers in Neuroscience. 2016; 9: 507. https://doi.org/10.3389/fnins.2015.00507
[40] Zhu D, Zhang S, Wang X, Xiao C, Cui G, Yang X. Secretory Clusterin Inhibits Dopamine Neuron Apoptosis in MPTP Mice by Preserving Autophagy Activity. Neuroscience. 2024; 540: 38–47. https://doi.org/10.1016/j.neuroscience.2024.01.010
[41] Pang J, Vince JE. The role of caspase-8 in inflammatory signalling and pyroptotic cell death. Seminars in Immunology. 2023; 70: 101832. https://doi.org/10.1016/j.smim.2023.101832
[42] García-Revilla J, Ruiz R, Espinosa-Oliva AM, Santiago M, García-Domínguez I, Camprubí-Ferrer L, et al. Dopaminergic neurons lacking Caspase-3 avoid apoptosis but undergo necrosis after MPTP treatment inducing a Galectin-3-dependent selective microglial phagocytic response. Cell Death & Disease. 2024; 15: 625. https://doi.org/10.1038/s41419-024-07014-9
[43] Shi Y, Wang H, Chen J, Ren J, Sun X, Qu M, et al. α-Synuclein Deletion Leads to Hyposmia: due to Defective Autophagy Induced by Abnormal PI3K/mTOR Signaling Pathway in Olfactory Bulb. Molecular Neurobiology. 2026; 63: 378. https://doi.org/10.1007/s12035-026-05686-2
[44] Soni R, Shah J. Unveiling the significance of synaptic proteins in parkinson's pathogenesis: A review. International Journal of Biological Macromolecules. 2025; 304: 140789. https://doi.org/10.1016/j.ijbiomac.2025.140789
[45] Park TY, Jeon J, Cha Y, Kim KS. Past, present, and future of cell replacement therapy for parkinson's disease: a novel emphasis on host immune responses. Cell Research. 2024; 34: 479–492. https://doi.org/10.1038/s41422-024-00971-y
[46] Coukos R, Krainc D. Key genes and convergent pathogenic mechanisms in Parkinson disease. Nature Reviews. Neuroscience. 2024; 25: 393–413. https://doi.org/10.1038/s41583-024-00812-2
[47] Morris HR, Spillantini MG, Sue CM, Williams-Gray CH. The pathogenesis of Parkinson's disease. Lancet (London, England). 2024; 403: 293–304. https://doi.org/10.1016/S0140-6736(23)01478-2
[48] Trenkwalder C, Mollenhauer B. The long road to neuroprotection for Parkinson's disease. The Lancet. Neurology. 2024; 23: 2–3. https://doi.org/10.1016/S1474-4422(23)00462-3
[49] Deliz JR, Tanner CM, Gonzalez-Latapi P. Epidemiology of Parkinson's Disease: An Update. Current Neurology and Neuroscience Reports. 2024; 24: 163–179. https://doi.org/10.1007/s11910-024-01339-w
[50] Yao L, Chen R, Zheng Z, Hatami M, Koc S, Wang X, et al. Translational evaluation of metabolic risk factors impacting DBS efficacy for PD-related sleep and depressive disorders: preclinical, prospective and cohort studies. International Journal of Surgery (London, England). 2025; 111: 543–566. https://doi.org/10.1097/JS9.0000000000002081
[51] Gu Y, He M, Zhou X, Liu J, Hou N, Bin T, et al. Endogenous IL-6 of mesenchymal stem cell improves behavioral outcome of hypoxic-ischemic brain damage neonatal rats by supressing apoptosis in astrocyte. Scientific Reports. 2016; 6: 18587. https://doi.org/10.1038/srep18587
[52] Huang J, U KP, Yang F, Ji Z, Lin J, Weng Z, et al. Human pluripotent stem cell-derived ectomesenchymal stromal cells promote more robust functional recovery than umbilical cord-derived mesenchymal stromal cells after hypoxic-ischaemic brain damage. Theranostics. 2022; 12: 143–166. https://doi.org/10.7150/thno.57234
[53] Teli P, Nachanekar A, Kale V, Vaidya A. Priming mesenchymal stromal cells with neurotrophic factors boosts the neuro-regenerative potential of their secretome. Regenerative Medicine. 2023; 18: 329–346. https://doi.org/10.2217/rme-2022-0201
[54] Shakespear N, Ogura M, Yamaki J, Homma Y. Astrocyte-Derived Exosomal microRNA miR-200a-3p Prevents MPP+-Induced Apoptotic Cell Death Through Down-Regulation of MKK4. Neurochemical Research. 2020; 45: 1020–1033. https://doi.org/10.1007/s11064-020-02977-5
[55] Luo S, Sun X, Huang M, Ma Q, Du L, Cui Y. Enhanced Neuroprotective Effects of Epicatechin Gallate Encapsulated by Bovine Milk-Derived Exosomes against Parkinson's Disease through Antiapoptosis and Antimitophagy. Journal of Agricultural and Food Chemistry. 2021; 69: 5134–5143. https://doi.org/10.1021/acs.jafc.0c07658
[56] Mobahat M, Sadroddiny E, Nooshabadi VT, Ebrahimi-Barough S, Goodarzi A, Malekshahi ZV, et al. Curcumin-loaded human endometrial stem cells derived exosomes as an effective carrier to suppress alpha-synuclein aggregates in 6OHDA-induced Parkinson's disease mouse model. Cell and Tissue Banking. 2023; 24: 75–91. https://doi.org/10.1007/s10561-022-10008-6
[57] Foltynie T, Bruno V, Fox S, Kühn AA, Lindop F, Lees AJ. Medical, surgical, and physical treatments for Parkinson's disease. Lancet (London, England). 2024; 403: 305–324. https://doi.org/10.1016/S0140-6736(23)01429-0
[58] Postuma RB, Lang AE. The Clinical Diagnosis of Parkinson's Disease-We Are Getting Better. Movement Disorders : Official Journal of the Movement Disorder Society. 2023; 38: 515–517. https://doi.org/10.1002/mds.29319
[59] Dong-Chen X, Yong C, Yang X, Chen-Yu S, Li-Hua P. Signaling pathways in Parkinson's disease: molecular mechanisms and therapeutic interventions. Signal Transduction and Targeted Therapy. 2023; 8: 73. https://doi.org/10.1038/s41392-023-01353-3